

Computer simulation for hybrid plenoptic camera super-resolution refocusing with focused and unfocused mode

Zhang Wei^{1,2}, Guo Xin¹, You Suping¹, Yang Bo¹, Wan Xinjun¹

(1. Engineering Research Center of Optical Instrument and System, Ministry of Education, Shanghai Key Lab of Modern Optical System, School of Optical-Electrical and Computer Engineering, University of Shanghai for Science and Technology, Shanghai 200093, China;

2. State Key Laboratory of Transient Optics and Photonics, Chinese Academy of Sciences, Xi'an 710119, China)

Abstract: Light field is a representation of full four-dimensional radiance of rays in free space. Plenoptic camera is a kind of system which could obtain light field image. In typical plenoptic camera, the final spatial resolution of the image is limited by the numbers of the microlens of the array. The focused plenoptic camera could capture a light field with higher spatial resolution than the traditional approach, but the directional resolution will be decreased for trading. Two models were set up to emulate the 4D light field distribution in both the traditional plenoptic camera and the focused plenoptic camera respectively. The 4D light field images of the two kinds of plenoptic camera were simulated by the software ZEMAX. The differences of sampling methods of the two kinds of plenoptic camera were analyzed. A variable focal length microlens array was presumed to be used in plenoptic camera to implement both focused and unfocused light field imaging. Based on the recorded light field, the corresponding refocusing process was discussed then. The refocused images at different depth were calculated. A new method of enhancing the resolution of the refocused images by image fusion and super resolution theories was presented. A reconstructed all in-focus image with resolution of 3 times of traditional plenoptic camera and same depth of field was achieved finally.

Key words: light field camera; super-resolution; digital refocusing; variable focal length microlens array

CLC number: TB879 **Document code:** A **Article ID:** 1007-2276(2015)11-3384-09

混合式光场相机在聚焦与非聚焦模式下的超分辨重聚焦仿真

张 薇^{1,2}, 郭 鑫¹, 尤素萍¹, 杨 波¹, 万新军¹

(1. 上海理工大学 光电信息与计算机工程学院 光学仪器与系统教育部工程研究中心
上海市现代光学系统重点实验室, 上海 200093;

2. 中国科学院瞬态光学与光子技术国家重点实验, 陕西 西安 710119)

摘 要: 光场描述了光在自由空间传播的全四维信息, 光场相机可用来获得光场图像。在传统的光场

收稿日期: 2015-03-14; 修订日期: 2015-04-19

基金项目: 国家自然科学基金(61205015, 61108051); 高等学校博士学科点专项科研基金优先发展领域课题(20123120130001);
国家重点实验室开发基金(SKLST201308); 上海市重点学科项目第三期项目(S30502);
国家重大科学仪器设备开发专项项目(2012YQ170004)

作者简介: 张薇(1978-), 女, 副教授, 博士, 主要从事光学系统设计、图像处理等方面的研究。Email: wei_zhang@usst.edu.cn

相机中,最终获得图像的空间分辨率受限于微透镜阵列中透镜的个数。聚焦型光场相机相较于传统光场相机能够获得更高的空间分辨率,但是以牺牲其角度分辨率作为代价。在 Zemax 中建立了传统光场相机与将聚焦光场相机的成像模型,仿真获得了两种光场相机的光场图像,分析了两种不同类型光场相机采样模式的区别。提出将可变焦液体透镜阵列放置在光场相机中,可以同时获得聚焦和非聚焦两种模式下的光场图像。根据记录的光场信息,讨论了相应的重聚焦方法,计算仿真了在不同景深下的重聚焦图像,并提出了一种基于图像融合和超分辨率重构的方法来提高重聚焦图像的分辨率,最终在相同的景深范围内获得了 3 倍于传统光场相机分辨率的重聚焦图像。

关键词:光场相机; 超分辨; 数字重聚焦; 可变焦液体透镜阵列

0 Introduction

A conventional imaging action translates a 3D scene to its 2D projection. During this imaging process, the depth information of the scene will be lost. Recently, researchers have developed a new imaging system which is referred to as plenoptic camera. Unlike a conventional camera, plenoptic camera can record information regarding light field and achieve a fully 3D photograph by post imaging processing. Light field image enables many new potential developments and promising applications, such as digital refocusing, aberration correction, 3D display and so on.

The fundamental ideas behind 3D photography can be traced back to Lippmann's and Ives' early 20th century works. As an application of 3D photography, plenoptic was proposed by Adelson-Wang^[1] and implemented by Ng^[2]. In Ng's plenoptic camera model, it inserts a lens array into a conventional camera to capture both angular and spatial distribution of light rays. The spatial resolution of the final image is limited by the number of the micro lens in the array. After Ng's plenoptic camera model, Lumsdaine et al. proposed a focused plenoptic camera model and its rendering method^[3-6], which would have higher spatial resolution than Ng's, but lower directional resolution for trading. The problems of the trading off spatial vs. angular sampling were discussed in^[7].

In this paper, a new hybrid plenoptic camera system which can work both on unfocused mode

(traditional mode) and focused mode is proposed. A variable focal length microlens array is presumed to be used in this system. By setting simple adjustment, the system can capture both unfocused light field image and focused light field image. This hybrid plenoptic camera can provide flexible light field imaging that can be varied between a high spatial resolution camera and a great refocusing power camera by choosing of user for different requirements. Based on the recorded light field data, the refocused images at different depth in both working modes are calculated and compared. Finally, an all in-focus image with 3 times spatial resolution of the traditional light field camera and similar depths of field is reconstructed by combining a set of images focused at different depths calculated in both working modes.

The remainder of this paper is organized as follows. Section 1 gives the basic equations of ray transfer matrices of the unfocused and focused light field camera separately, and compares the different sampling modes of them. Section 2 gives the configuration of a hybrid plenoptic system, and introduces the work process of the system. A simulation is accomplished by establishing the hybrid plenoptic camera in ZEMAX software. The light field images are simulated and the refocusing images are computed in both two kinds of working mode. A final image with both high spatial resolution and large depth of field is obtained by combining the images achieved in two working modes. Section 3 concludes this paper and proposes some possible work in the future.

1 Ray transfer and simpling pattern

1.1 Unfocused plenoptic camera

An unfocused plenoptic camera is illustrated in Fig.1, which consists of a main lens and a microlens array placed in front of a sensor. The distance

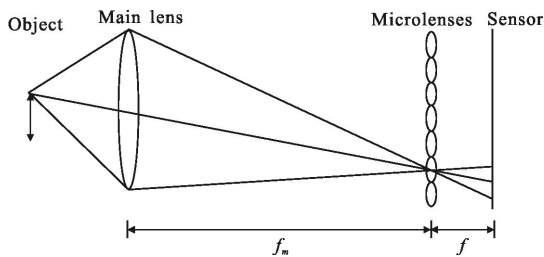


Fig.1 Unfocused plenoptic camera

between the main lens and the microlens array is f_m , which is equivalent to the focal length of the main lens. The distance between the microlens and the sensor is f , which is the focal length of each microlens. The main lens is focused at the microlens plane and the microlenses are focused at optical infinity. The diameter of each microlens is d .

Without loss of generality, a two-dimensional plane is only discussed. The light field can be represented by a density function $R(u, s)$, where u is the position, and s is the direction of the incident ray. The pair (u, s) can also be rewritten as one vector x . Since the radiance through optical system is assumed to be conserved, we have:

$$R'(x')=R(x) \tag{1}$$

For any optical transformation A , the rays transformation is according to $x'=Ax$ or $x=A^{-1}x'$. Then we have the following for the operation of optical transformations on radiance:

$$R'(x)=R(A^{-1}x) \tag{2}$$

When an image is captured on a sensor, the intensity at a given point of the image is the integral over all directions for the radiance at that point, which can be represented as:

$$I(u)=\int_s R(u, s)ds \tag{3}$$

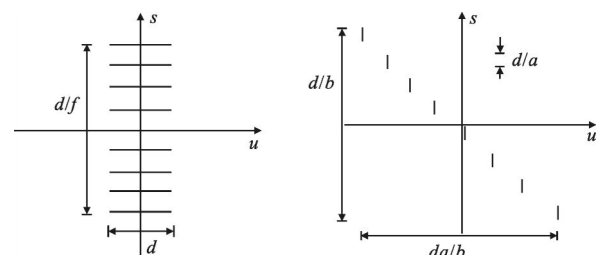
In an unfocused plenoptic camera, rays incident from the main lens to one microlens, and then propagate a distance f to the sensor. The radiance at the microlens plane and at the sensor plane are represented as R_m and R_s respectively. According to the Matrix Optics, the process can be written as:

$$R_m(x)=R_s(A^{-1}x) \tag{4}$$

where $A=\begin{bmatrix} 1 & f \\ 0 & 1 \end{bmatrix} \begin{bmatrix} 1 & 0 \\ -\frac{1}{f} & 1 \end{bmatrix} = \begin{bmatrix} 0 & f \\ -\frac{1}{f} & 1 \end{bmatrix}$, $A^{-1}=\begin{bmatrix} 1 & -f \\ \frac{1}{f} & 0 \end{bmatrix}$.

According to the Eq.(4), a pixel on the sensor samples a single direction in the directional coordinate and a span of d in the positional coordinate, where the d is the diameter of each microlens. A microlens samples one position in the positional coordinate and a span of d/f in the directional coordinate. The sampling mode is shown in Fig.2(a).

It can be seen that in an unfocused plenoptic camera, the directional resolution depends on the number of the pixels behind one microlens, while the spatial resolution depends on the number of the microlenses. Limited by the number of the microlenses, images rendered by the radiance captured by the unfocused plenoptic camera have very low resolution. And this is the biggest drawback for the unfocused plenoptic camera.



(a) Sampling pattern in unfocused plenoptic camera (b) Sampling pattern in focused plenoptic camera

Fig.2 Schematic of sampling patterns of the two kinds of plenoptic camera

1.2 Focused plenoptic camera

In a focused plenoptic camera, the microlens array is inserted behind (or in front of) the focal

plane of the main lens at a distance of a , instead of being put into the location of the main lens' focal plane. And the distance between the microlens and the sensor is b instead of f , which is the focal length of each microlens, as shown in Fig.3. The a and b should satisfy the lens equation, $1/a+1/b=1/f$.

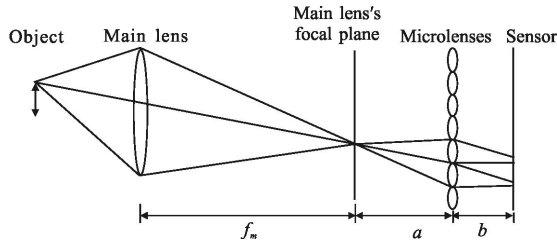


Fig.3 Focused plenoptic camera

Without loss of generality, we suppose that the microlens array is behind the focal plane of the main lens and $b > f$. In this case, a real image is captured on the sensor. The radiance at the focal plane of the main lens is secondly imaged at the sensor by the microlens. Suppose the radiance at the focal plane of the main lens is R_f , and the radiance at the sensor plane is R_s . According to the Matrix Optics, we have:

$$R_f(x) = R_s(A^{-1}x) \quad (5)$$

where $A = \begin{bmatrix} 1 & b \\ 0 & 1 \end{bmatrix} \begin{bmatrix} 1 & 0 \\ \frac{1}{f} & 1 \end{bmatrix} \begin{bmatrix} 1 & a \\ 0 & 1 \end{bmatrix} = \begin{bmatrix} -\frac{b}{a} & 0 \\ -\frac{1}{f} & -\frac{a}{b} \end{bmatrix}$, $A^{-1} = \begin{bmatrix} -\frac{b}{a} & 0 \\ \frac{1}{f} & -\frac{a}{b} \end{bmatrix}$.

Consider the Eq. (5), a pixel on the sensor samples a span of d/a in the direction coordinate and a single position in the position coordinate. Each microlens samples a span of da/b in the position coordinate and a span of dlb in the direction coordinate. The sampling pattern is shown in Fig.2 (b). Then it can be seen that the spatial resolution of a focused plenoptic camera depends on not the number of the microlenses but the resolution of the microlens image. In this way, the spatial resolution is enhanced while

the directional resolution is decreased for trading. In focused plenoptic camera, the different focal plane in the scene will have different resolution. The best spatial resolution is increased to b/a times the resolution of the sensor image, while the angular resolution is limited in a/b .

2 System configuration and image rendering

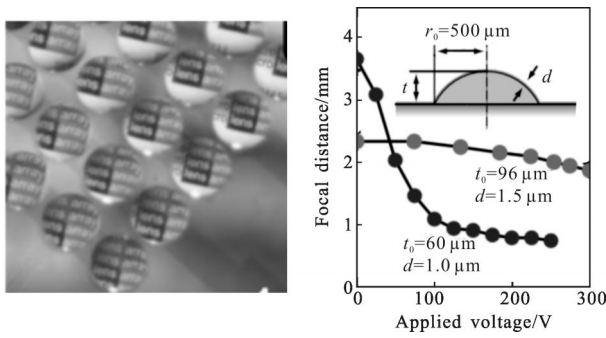
2.1 Configuration of hybrid plenoptic camera

Since the focused plenoptic camera can get higher spatial resolution while the unfocused plenoptic camera can get better directional resolution, is there any way to combine these two patterns and render an image with both higher spatial and directional resolution? The main objective here is to design a hybrid system which can implement both focused and unfocused light field image capturing.

2.1.1 Variable focal length microlens array

Liquid lens is a novel optical device which can implement active zooming. It has a very wide potential application in many fields. There are many kinds of liquid lens technology^[8-11]. Nguyen presented a method to fabricate a variable focal length liquid lens by depositing parylene onto the surface of a liquid in a vacuum^[11]. The deposited parylene films take the form of a soft "skin" encapsulating a liquid droplet. The focal length of the liquid lens can be changed by adjusting the voltage added on the lens. By use of this method, the diameter of the liquid lens could have a very large range from 20 μm to 30 mm. And it can be used to build a varifocal microlens array conveniently. The schematic of this kind of varifocal lens array is shown in Fig.4.

By applying this varifocal microlens array, a hybrid plenoptic camera system is proposed. With simple adjustment, the system can work both on unfocused mode and focused mode, and capture both unfocused light field image and focused light field image.



(a) A array with 1 mm of each lens' diameter (b) Relationship between focal distance change and applied voltage

Fig.4 Schematic of varifocal microlens array^[11]

2.1.2 Hybrid plenoptic camera configuration

The configuration of hybrid plenoptic camera is shown in Fig.5. As shown in Fig.5 (a), the microlens array is put into the location of the main lens' focal plane. And the distance between the microlens array and the sensor is fixed as f_1 , which is the initial focal length of each microlens. At this time, the system is working in the unfocused mode just like a traditional plenoptic camera.

Then the focal length of the varifocal microlens tunes to f_2 and the system turns to the focused mode, as shown in Fig.5 (b) and (c). Because of the microlens' focal length changing, the sensor is not on the focal plane of the microlens but at a special distance of $b=f_1$. For a single microlens, there is a conjugate distance can be calculated from the lens equation: $1/a+1/b=1/f_2$. Then we get:

$$a = \frac{f_2 b}{b - f_2} = \frac{f_2 f_1}{f_1 - f_2} \tag{6}$$

It can be seen from the Eq.(6) that there is a plane B' (shown as B_1' in Fig.5(b), and B_2' in Fig.5(c)) after the microlens array at distance of a is imaged at the sensor plane, which is conjugate with a plane B (shown as B_1 in Fig.5(b), and B_2 in Fig.5(c)) in the objective space through the main lens. We can interpret this process as following: An object on the B plane is imaged at B' plane (shown as dashes in Fig.5) by the main lens. Then it is conjugate with the sensor

plane through the microlenses. In the case of $f_1 < f_2$, as shown in Fig.5(c), a is negative and B_2' plane is after the sensor plane, which means the image created by the main lens is virtual and is re-imaged onto the sensor by the microlenses. The highest resolution is achieved on the object plane which is closer to the main lens compared with the unfocused mode condition. In the other case: $f_1 > f_2$, as shown in Fig.5(b), a is positive and B_1' plane is in front of the microlens plane, which means the main lens creates a real image at this plane. The highest resolution is achieved on the object plane which is farther from the main lens compared with the unfocused mode condition. We choose $f_1 < f_2$ in the hybrid plenoptic camera model, because the microlens' image will be enlarged and cause overlap on the condition of $f_1 > f_2$.

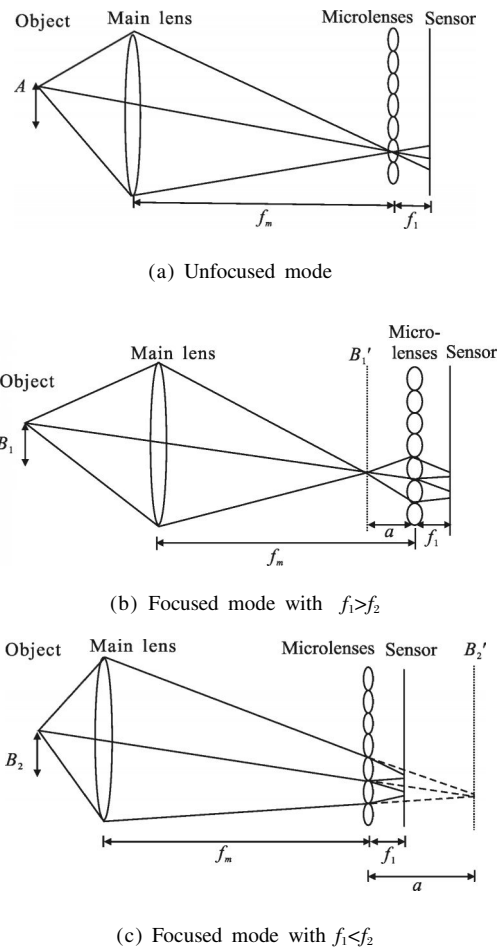


Fig.5 Configuration of hybrid plenoptic camera

We define β to be the ratio of the two focal

length, which can be written as $\beta=f_1/f_2$. Since $f_1<f_2$ in our hybrid plenoptic camera model, we know that $0<\beta<1$. The highest spatial resolution can be obtained is $(1-\beta)$ times of the resolution of the sensor image. The depth plane with the highest spatial resolution can be calculated by the Eq.(7):

$$F_{\text{res}}=F+\frac{\beta}{(1-\beta)}f_2 \quad (7)$$

where F is the depth of the microlens plane.

2.2 Image rendering

As the analysis in section 2, rendering for a finite size aperture image requires integration in the angular dimension at the same spatial point. In the unfocused mode, a same spatial point is within a microlens image, but it is cross microlens images in the focused mode. For hybrid plenoptic camera, the different depth images are refocused by shifting and adding the sub-aperture images in the unfocused mode, which also can be computed in the Fourier domain by Fourier slice technology^[3]. In the focused mode, the different depths images are reconstructed by selecting different patch size and averaging together the same spatial point^[5]. Because the depth in the focused mode is limited by a/b , which is equivalent to $1/(1-\beta)$, the extendable depth of field is smaller than that is in the unfocused mode. The images refocused at all depths in both modes create a focal stack of images. Then an all in-focus image can be computed by some algorithms for extending the depth of field from a set of images focused at different depths, such as digital photomontage technology^[12]. Notice that before digital photomontage, each different depth image should be of the same resolution. We can realize this by interpolation or down sampling. Since the resolution of the images computed in the unfocused mode is smaller than the final reconstructed image, we can use a super-resolution processing on the sub-aperture images to get higher spatial resolution^[13-14]. After all this processes, we get an final image with the spatial resolution as high as a focused plenoptic but with lager depth of

field. The image rendering process is shown in Fig.6.

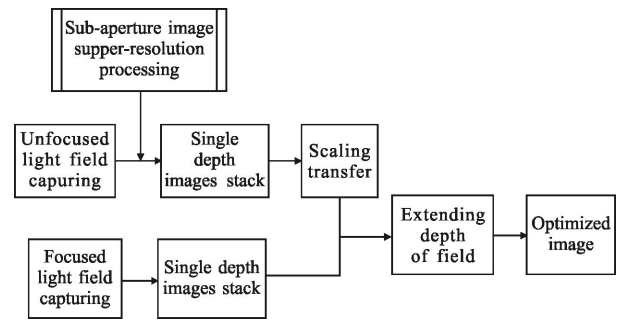


Fig.6 Flow chart of image rendering process of hybrid plenoptic system

2.3 Simulation implementation

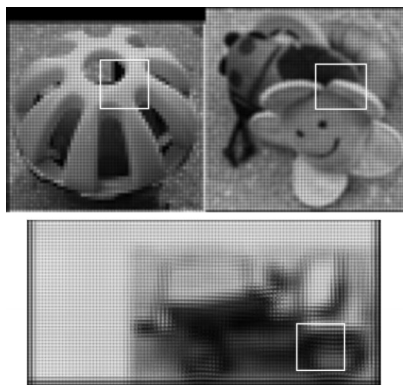
To demonstrate the hybrid plenoptic camera imaging, we implemented the simulation using a hybrid plenoptic camera established in ZEMAX software. We design three scenes with a single plane target at different distance from the main lens. The first target is a picture of rattle which is put at the position of the optical focus of the main lens. The second target is a sunflower toy which is closer to the main lens than the rattle. And the third target is a toy car which is farther from the main lens than the rattle. In the simulation the microlens array consists of 300×300 circular lenses with pitch of 0.125 mm. The initial focal length of each microlens is 0.5 mm which is used in the unfocused mode. The microlens array locates at the distance of 156.9 mm behind the main lens. A photosensor with $4\ 500\times 4\ 500$ pixels is placed at the focal plane of the microlenses. The pixel pitch is $8.3\ \mu\text{m}$, indicating that each microlens covers 15×15 pixels behind. Since we don't think of the effect of the aberrations of system here, a perfect lens is used as the main lens. A summarizing of the overall parameters in the simulation is shown in Tab.1.

After capturing the light field image in the unfocused mode, the system is simulated as working in the focused mode. The objective distance is not changed in the both working modes. The focal length of the microlens is varied from f_1 to f_2 .

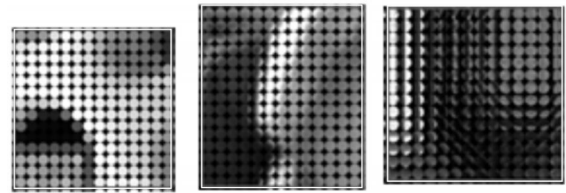
Tab.1 Configuration of the simulated plenoptic camera and the position of each single plane target

Item	Parameter	Value
Objective distance	Rattle	1300 mm
	Sunflower toy	1148 mm
	Toy car	1470 mm
Main lens	Focal length	140 mm
	$F\#$	4
	Focal length f_1	0.5 mm
	Focal length f_2	0.625 mm
Microlens array	$\beta=f_1/f_2$	0.8
	Diameter	0.125 mm
	Number	300×300
Sensor	Pixel size	8.3 μm
	Pixel number	4 500×4 500

Figure 7 shows the light field image simulated in the unfocused mode and its refocusing results, while Fig.8 shows the image simulated in the focused mode and its refocusing results. Fig.8(b) is calculated based on the basic rendering algorithm^[6]. From Fig.7(c), it can be seen that the refocusing results of the three targets are of low resolution. But they are as clear as each other. On the contrary, it can be seen from Fig.8(b) that the sunflower toy is much clearer than the rattle and the toy car. Especially the toy car is



(a) 4-D light field image captured by the system

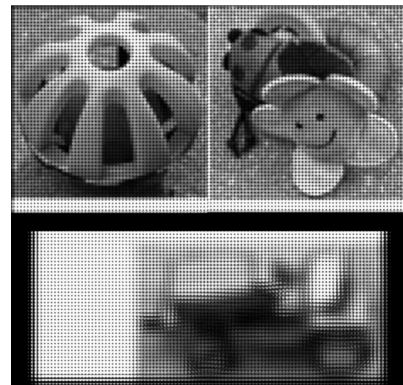


(b) Amplified images of the areas in the red box of (a)

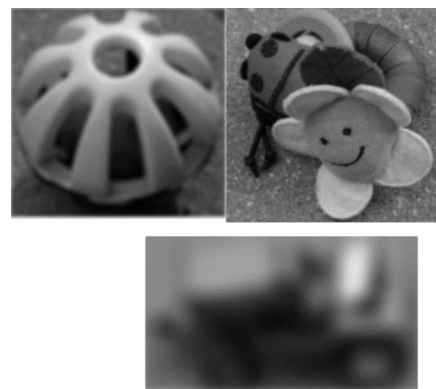


(c) Refocusing results calculated by Fourier slice technology

Fig.7 Simulated results in the unfocused mode



(a) 4-D light field image captured by the system



(b) Refocusing results calculated based on the basic rendering algorithm

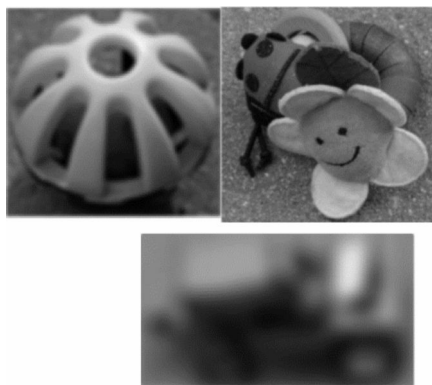
Fig.8 Simulated results in the focused mode

almost can't be recognized. It means that the resolution is much sensitive to the depth of field in the focused mode.

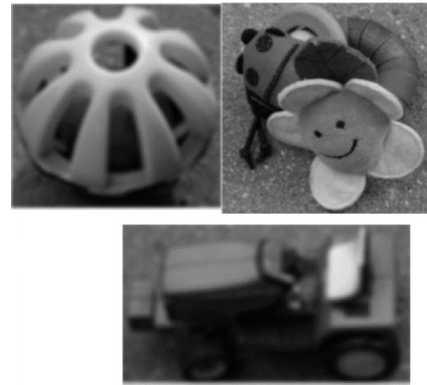
Figure 9 shows the comparison of the two refocusing images and a final image combined by them. In order to compare these two refocusing results, we computed the images with same pixels 900×900 , which is the best resolution in the focused mode. Since we only use three single plane targets in the simulation, the final image with all depths of field can be obtained by choosing the better one in the refocusing results of the three targets computed in the two kinds of working mode, and combining them directly. But in an actual scene, it is impossible to combine those images by such a simple way. Some algorithms such as digital photomontage should be used to reconstruct the final image. It can be seen from Fig.9 (c) that the final reconstructed image has both higher spatial resolution and larger depths of field.



(a) Bilinearly interpolated refocusing image calculated in the unfocused mode



(b) Refocusing image computed in the focused mode



(c) Final reconstructed image

Fig.9 Refocusing images of the two working modes and the final image combined by them

3 Conclusion

Plenoptic cameras can record 4-D light field information that can be used in digital refocusing, depth field extending, aberration correction, and 3-D display ... There are two kinds of plenoptic camera which are unfocused(traditional) and focused plenoptic camera. The sampling modes of the two kinds of plenoptic camera are different. The unfocused plenoptic camera has high directional resolution but low spatial resolution; on the contrary, the focused light field camera has high spatial resolution but low directional resolution. In this paper, a way to build a hybrid plenoptic camera by application of variable focal length microlens array is presented. The focal length of each microlens can be varied by adjusting the voltage added on them. By changing the focal length of the microlens, the hybrid plenoptic camera can work in both unfocused and focused mode. This hybrid plenoptic has many advantages. It provides a flexible light field imaging application that can be varied between a camera with higher spatial resolution and a camera with greater refocusing power, which can be chosen by user for different cases. And it also provides a way to render images from light field information with both high spatial and directional resolution. We simulate a way to reconstruct an image

whose spatial resolution is 3 times of the number of the microlens, which is the limitation of the spatial resolution in unfocused mode, and the depth of field is larger than the image rendered only in the focused mode. A prototype of the hybrid plenoptic camera will be built soon after.

In this paper, the image rendering process is separated during the two kinds of working mode. The final image is achieved by combining the better results of the single depth images stacks obtained by the two separated process. But the algorithm of how to reconstruct the final image between the two 4-D light field imaging should be studied in the future work.

References:

- [1] Adelson T, Wang J. Single lens stereo with a plenoptic camera [J]. *IEEE*, 1992, 14(2): 99–106.
- [2] Ng R. Digital lightfield photography [D]. CA, USA: Stanford University, 2006.
- [3] Ng R. Fourier slice photography [J]. *ACM Transactions on Graphics*, 2005, 24(3): 735–744.
- [4] Lumsdaine A, Georgiev T. The focused plenoptic camera [J]. *Computational Photography (ICCP), IEEE*, 2009: 1–8.
- [5] Georgiev T, Lumsdaine A. Focused plenoptic camera and rendering [J]. *Journal of Electronic Imaging*, 2010, 19(2): 021106.
- [6] Lumsdaine A, Georgiev T. Full resolution light field rendering [R]. USA: Adobe Systems, 2008.
- [7] Georgiev T, Zheng K, Curless B, et al. Spatio-angular resolution trade off in integral photography [R]. Eurographics Symposium on Rendering, 2006.
- [8] Kuiper S, Hendriks B H W. Variable-focus lens for miniature cameras [J]. *Appl Phys Letter*, 2004, 85(7): 100–109.
- [9] Lee S W, Lee S S. Focal tunable liquid lens integrated with an electromagnetic actuator [J]. *Appl Phys Letter*, 2007, 90(12): 121129–121131.
- [10] Ren H, Wu S. Variable-focus liquid lens by changing aperture [J]. *Appl Phys Letter*, 2005, 86(21): 211107–211109.
- [11] Binh-Khiem N, Matsumoto K, Shimoyama I. Polymer thin film deposited on liquid for varifocal encapsulated liquid lenses [J]. *Appl Phys Letter*, 2008, 93(12): 124101–124103.
- [12] Agarwala A, Dontcheva A, Agrawala M, et al. Interactive digital photomontage [J]. *ACM Transactions on Graphics*, 2004, 23(3): 294–302.
- [13] Mendlovic D. Toward a super imaging system [J]. *Applied Optics*, 2013, 52(4): 561–566.
- [14] Park S C, Park M K, Kang M G. Super-resolution image reconstruction: A technical overview [J]. *IEEE Signal Processing Magazine*, 2003, 20(3): 21–36.